frontiers in Energy Research

ORIGINAL RESEARCH
published: 03 November 2021
doi: 10.3389/fenrg.2021.787237

An Ultra-High Temperature Stable Solar Absorber Using the ZrC-Based Cermets

Jian Wang[1], Zuoxu Wu[1], Yijie Liu[1], Shuaihang Hou[2], Zhikun Ren[1], Yi Luo[1], Xingjun Liu[2], Jun Mao[2], Qian Zhang[2] and Feng Cao[1]**

[1]School of Science, And Ministry of Industry and Information Technology Key Lab of Micro-Nano Optoelectronic Information System, Harbin Institute of Technology, Shenzhen, China, [2]School of Materials Science and Engineering, And Institute of Materials Genome and Big Data, Harbin Institute of Technology, Shenzhen, China

Exploring the spectrally selective absorbers with high optical performance and excellent thermal stability is crucial to improve the conversion efficiency of solar energy to electricity in concentrated solar power (CSP) systems. However, there are limited reports on the selective solar absorbers utilized at 900°C or above. Herein, we developed a selective absorption coating based on the ultra-high temperature ceramic ZrC and the quasi-optical microcavity (QOM) optical structure, and experimentally achieved the absorber *via* depositing an all-ceramic multilayer films on a stainless steel substrate by magnetron sputtering. The prepared multi-layer selective absorber demonstrates an excellent high solar absorptance of ~0.964 due to the multi absorptance mechanisms in the QOM, and a relatively low thermal emittance of ~0.16 (82°C). Moreover, the coating can survive at 900°C in vacuum for 100 h with a superior spectral selectivity of 0.96/0.143 (82°C) upon annealing, resulting from the introduction of ultra-high temperature ceramic ZrC in the QOM structure. Under the conditions of a stable operating temperature of 900°C and a concentration ratio of 1,000 suns, the calculated ideal conversion efficiency using this absorber can reach around 68%, exceeding most solar selective absorbers in previous reports.

Keywords: solar selective absorption coatings1, ultra-high temperature ceramics2, ZrC-Al_2O_3 composite3, thermal stability4, total efficiency5

OPEN ACCESS

Edited by:
K. Sudhakar,
Universiti Malaysia Pahang, Malaysia

Reviewed by:
Kumaran Kadirgama,
Universiti Malaysia Pahang, Malaysia
Xiang-Hu Gao,
Lanzhou Institute of Chemical Physics (CAS), China

****Correspondence:***
Qian Zhang
zhangqf@hit.edu.cn
Feng Cao
caofeng@hit.edu.cn

Specialty section:
This article was submitted to Solar Energy, a section of the journal Frontiers in Energy Research

Received: *30 September 2021*
Accepted: *20 October 2021*
Published: *03 November 2021*

Citation:
Wang J, Wu Z, Liu Y, Hou S, Ren Z, Luo Y, Liu X, Mao J, Zhang Q and Cao F (2021) An Ultra-High Temperature Stable Solar Absorber Using the ZrC-Based Cermets. Front. Energy Res. 9:787237. doi: 10.3389/fenrg.2021.787237

INTRODUCTION

Over the past decades, to alleviate the increasingly severe fossil energy crisis, the capture and utilization of abundant solar energy have evolved into a hot research topic (Wu et al., 2021; Jiasheng 1996; Weinstein, Loomis, and Chen 2015). The photothermal conversion is a potential way to efficiently utilize the solar energy among various solar energy utilization methods including photoelectric (Chirumamilla et al., 2021; Wei et al., 2020; Wang S. et al., 2021), photothermal conversion (Hoch et al., 2016; Azad et al., 2016) and photobiological conversion (Rosenbaum et al., 2005; Turon et al., 2021). Compared with commercialized photovoltaic technologies, concentrated solar power (CSP) systems can overcome the problem of intermittent sunlight, but the high cost still hinders the large deployment (Yushchenko et al., 2018). The solar selective absorption coatings (SSACs), the core component of the CSP system, can substantially improve the solar to power conversion efficiency and enable the reduction of the levelized cost of energy (LCOE) of CSP systems (Kan et al., 2021) when the reliable operating temperature can reach or even exceed 750°C

TABLE 1 | The basic information about the used targets and substrate in the QOM-based absorber (CAA).

Materials	ZrC target	Al_2O_3 target	SiO_2 target	SS 304
Size	Φ50.8 mm × 4 mm	Φ50.8 mm × 4 mm	Φ50.8 mm × 4 mm	20 mm × 20 mm × 1 mm
Purity	99.95%	99.99%	99.99%	_

TABLE 2 | The deposition parameters of the coatings including composite ceramic layers (C1, C2, and C3) with different ZrC volume ratios in Al_2O_3, ZrC infrared (IR) layer, Al_2O_3, SiO_2, and CAA[a].

Sample	Substrate	ZrC	C1, C2 or C3	ZrC	C3	SiO_2
C1	Si	-	(C1) 96 nm	-	-	-
C2	Si	-	(C2) 110 nm	-	-	-
C3	Si	-	(C3) 103 nm	-	-	-
CAA	Si or SS	100 nm	(C3) 30 nm	25 nm	40 nm	70 nm

[a]*All the work in this paper was carried out in an Ar environment under a pressure of 0.4 Pa using the RF sputtering at room temperature.*

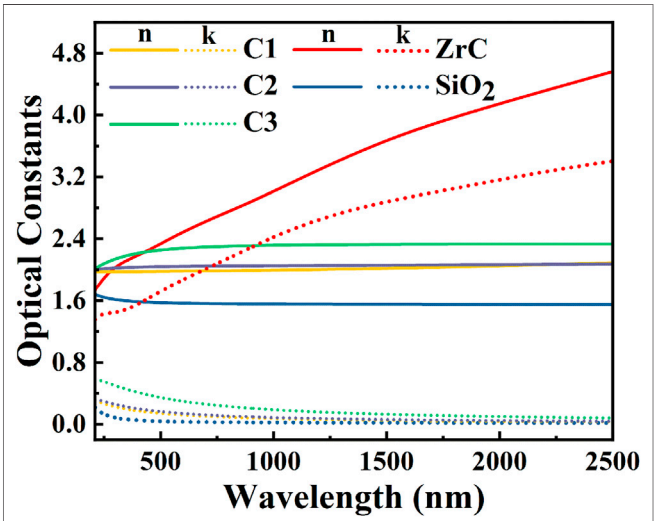

FIGURE 1 | Refractive index (n) and extinction coefficient (k) of ZrC, SiO_2, and ZrC-Al_2O_3 ceramic composites (C1, C2, and C3) with different volume ratios.

(Wang X. et al., 2021). Furthermore, the ultra-high solar absorptance in solar spectrum range and low thermal emittance in the thermal infrared regime are beneficial to realize high efficiency and low LCOE of CSP system (Vidal and Klammer 2019).

Various attempts (He et al., 2021a; Yang et al., 2020; He et al., 2021b) have been made but fulfilling the reliable operation of the absorber at high temperatures remains a challenge. So far, cermet-based absorbers composed of high-loss and refractory metals such as W, Ni, and Ta and the ceramic matrix have been extensively excavated (Liu et al., 2019; Ning et al., 2016; Cao et al., 2014). However, the thermal diffusion behavior of metal atoms at high temperatures will affect the light absorption of the coating and lead to optical degradation of the absorber. The strategy of metal alloying can effectively suppress the thermal diffusion phenomenon and then boost the stability of the absorber. Yang et al. utilized the TiW-SiO_2 as absorption layers to prepare SSACs on the quartz substrate. The experimental results showed that incorporating the second phase Ti could effectively improve the stability of the absorber (Yang et al., 2021). In addition, a series of binary alloys (WTa, WNi, TiC, etc) based selective absorbers were proposed and their stable operating temperatures were further enhanced (Cao et al., 2015a; Cao et al., 2015b; Wang et al., 2017; Wu et al., 2020). However, the reliable stable temperatures of these absorbers are below 750°C due to the limination of intrinsic material properties. In recent years, all-ceramic based absorbers have shown great potential for high-temperature applications, especially for absorbers with transition metal nitrides (Li et al., 2021; Meng et al., 2017; Liang et al., 2018) and their ceramic composites (Meng and Zhou 2019; Zhang et al., 2016; Cao et al., 2017) as the main absorption units realized by different optical designs and absorption mechanisms. Together with transition metal nitrides, transition metal carbides and borides also belong to the UHTCs, which are endowed with high melting temperature (≥3,000°C), good thermal and electrical conductivity (Chen et al., 2021), and chemical inertness (Tang and Hu 2017; Fahrenholtz and Hilmas 2017). Gao et al. utilized the UHTCs as the main absorption unit to design the selective absorbers, which can only maintain thermal stability below 600°C in vacuum (Gao et al., 2019b). The sophisticated optical design may hold promise in maximizing the material's advantages at high temperatures. Wu et al. raised a QOM structure based on W-SiO_2 cermet, which can enable the near-perfect light absorption by the interaction of multiple absorption mechanisms (Wu et al., 2019). However, the stable operating temperature is only 600°C. It is a feasible way to enhance the working temperature through incorporating the UHTCs in the QOM structure.

Herein, to overcome the thermal diffusion of metal atoms in the QOM structure at high temperature, we proposed a spectrally selective solar absorber based on the QOM optical structure and UHTCs. Combined with the optical properties of the materials, the solar selective absorbers with an ultra-high absorptance were obtained by the precise optimization design of the optical structure. Moreover, the prepared absorbers exhibit excellent thermal stability up to 900°C in vacuum, which is attributed to the introduction of ZrC in the QOM structure and the optimal design of ZrC in the composite ceramic layer. Near-perfect absorption over the broad solar spectrum and relatively low mid-IR emission could guarantee an ideal conversion efficiency of 68% in the CSP system. This developed strategy will also pave the way to designing the other ultra-high temperature absorbers.

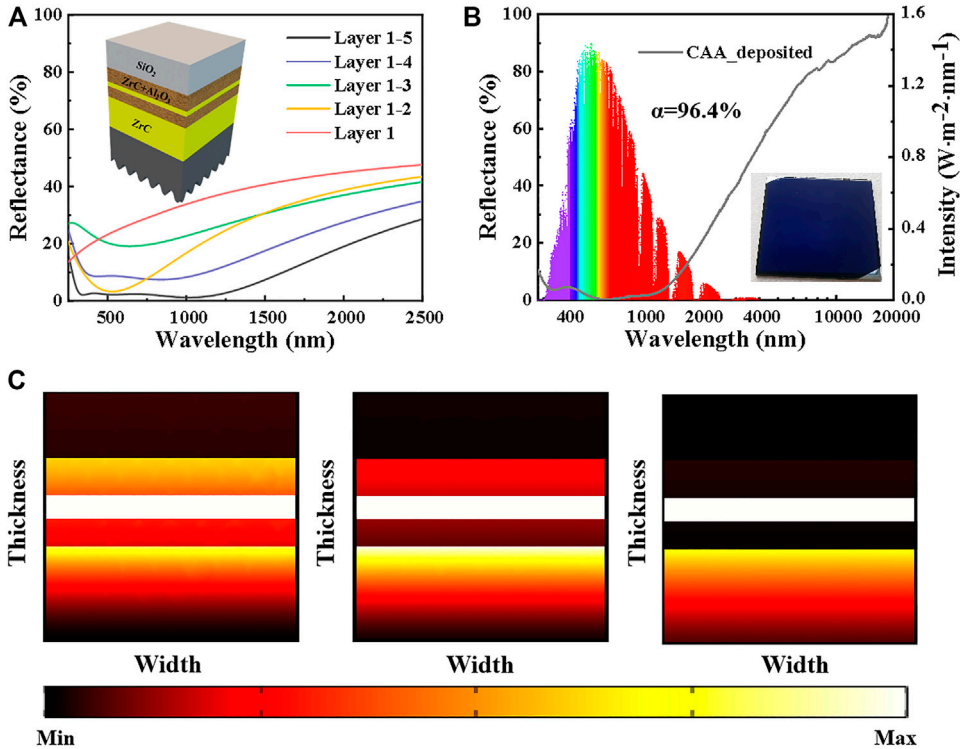

FIGURE 2 | (A) Simulated reflectance spectra of the layer-added coatings and the schematic of the optical structure. **(B)** The measured a reflection spectrum (gray line) the optical image of the CAA coating together with solar spectrum (AM 1.5, polychromatic block). **(C)** The distribution of electromagnetic power loss of the CAA at the wavelengths of 0.62, 1.11, and 2.5 μm, where λ = 0.62 μm is connected with the reflectance minimum.

MATERIALS AND METHODS

A commercial software (Essential Macleod) was used to optimize the optical structure. The different thresholds and weighted coefficients within the optimization region of 0.25–2.5 μm were set to realize the high solar absorptance. The optical constants of the individual layer involved in the optical design were measured by a spectroscopic ellipsometer (J. A. Woollam Co, Inc.). The designed ZrC-based spectral selective absorbers (CAA) were prepared by a high vacuum multi-target magnetron sputtering system (Beijing Technol Co. LTD, JCPY650) equipped with three high purity targets. Prior to the deposition, the polished stainless (SS304) substrates were cleaned successively with acetone and alcohol. More details about the used materials have been tabulated in the **Table 1**. All the coatings in this paper were carried out in an Ar environment under a pressure of 0.4 Pa using a radio frequency (RF) power at room temperature after the substrate bias cleaning for 10 min in the main chamber with the based pressure of below 4×10^{-4} Pa. By adjusting the sputtering power of ZrC target, three ZrC-Al_2O_3 composite ceramic layers (C1, C2, and C3) with different volume ratios of ZrC in composite layer were prepared *via* co-sputtering of ZrC and Al_2O_3. More details about the deposition parameters were summarized in **Table 2**.

The annealing tests were performed in a vacuum tube furnace at different target temperatures for 100 h with a heating rate of 5°C/ min. The vacuum pressure is about 4×10^{-2} Pa. The ultraviolet-visible-near infrared (0.28–2.5 μm) reflection spectra of the coatings were measured by a spectrophotometer (Agilent Cary 5,000) equipped with an integrating sphere, while the mid-IR reflection spectra in the wavelength range of 2.5–20 μm were collected by a Fourier transform infrared spectrometer (Nicolet IS50) equipped with a Pike Au integrating sphere at room temperature. The solar absorptance (α) and thermal emittance (ε) were calculated by the weighted integration of reflection spectra with the standard solar spectra and the black body emissive spectra, respectively (Wang J. et al., 2021).

The surface topographies were detected by an atomic force microscope (Oxford Instruments Asylum Research, Inc.) with a scanning area of 5 μm × 5 μm. The phase analysis of the samples was characterized by Raman spectra collected on a Raman spectrometer with a 532 nm laser excitation (Renishaw in *Via*) and XRD patterns obtained by a Rigaku diffractometer (LX-57B) with Cu-Kα radiation (40 kV, 200 mA, λ = 0.15406 nm).

RESULTS AND DISCUSSION

Optical Simulation and Absorption Mechanism Analysis of Solar Selective Absorption Coatings

To optimize the optical response of the CAA structure, we first measured the optical constants (n and k) of the materials used in

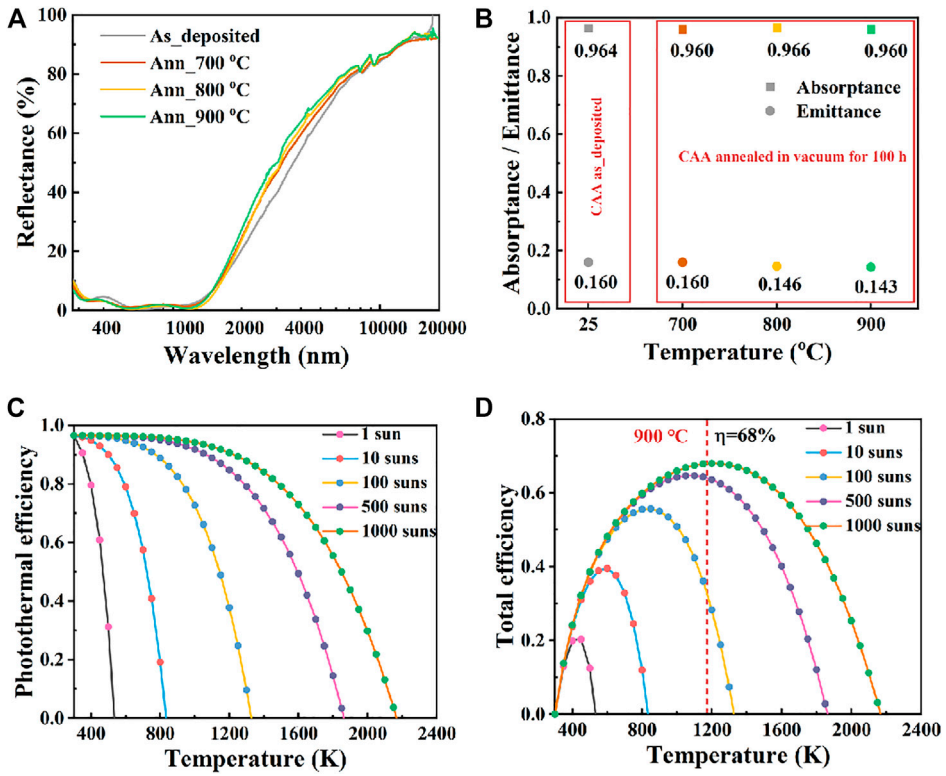

FIGURE 3 | (A) Reflection spectra of the coatings before (gray line) and after annealing in vacuum at 700°C (orange line), 800°C (yellow line), and 900°C (green line) for 100 h. **(B)** The solar absorptance and thermal emittance of the absorber under different heat treatment conditions. **(C)** Temperature-dependent photothermal efficiency with different optical concentrations. **(D)** Temperature-dependent total efficiency with different optical concentrations. The vertical red dotted line represents the temperatures of 900°C.

the structure, as shown in **Figure 1**. The Cauchy dispersion model was picked to fit the transparent material SiO_2, while Gen-Osc dispersion model including Cody-Lorentz and Gaussian oscillators was used to analyze the metallic ZrC and cermets (C1, C2, and C3). The larger extinction coefficient of ZrC confirms the intrinsic absorption due to the in-band contribution and the interband contribution of electrons (Okuhara et al., 2018). The SiO_2 demonstrates a near-constant refractive index and a near-zero extinction coefficient, which determines it can be used as the top anti-reflection coating. The composite ceramic layers (C1, C2, and C3) with different volume ratios of ZrC in Al_2O_3 matrix possess the optical constants with the values between SiO_2 and ZrC and present an increasing trend from 1.98 (C1) to 2.27 (C3), which indicates a substantial controlling space on the optical property *via* the modulation of the volume ratios of ZrC and Al_2O_3.

The QOM optical structure on the stainless-steel (SS) substrate with the coatings of ZrC/C3/ZrC/C3/SiO_2 from the bottom layer (layer 1) to the top layer (layer 5) was designed and shown in **Figure 2A**. The calculated reflectance spectra of the layer-added coatings (**Figure 2A**) demonstrate that the individual ZrC (layer 1) possesses moderate absorption due to the intrinsic spectral selectivity, and the absorption increases with adding more layers except for the bottom two layers (layer 1–2), which is ascribed to the introduction of ZrC middle layer (layer 3) enhancing the reflection on the coatings without another Z3 layer (layer 4) and the top ARC layer (layer 5). Eventually, the CAA (layer 1–5) exhibits a low reflectance of less than 5% in the wavelength range of 0.3–1.38 μm, indicating a superior absorptance. Therefore, we deposited the optimized CAA on the SS304 substrate, and the corresponding optical image and the reflectance spectra were shown in **Figure 2B**. The coating displays a blue appearance and a pretty low reflection across the solar spectrum range matched well with the calculated data. Multiple absorption mechanisms in the QOM structure contribute to the low reflectance in the solar spectrum region, while the bottom ZrC leads to high infrared reflectance, which jointly determines the excellent selective absorption of the prepared CAA coating. The reflectance minimum at 0.62 μm is attributed to the destructive interference of the interfaces (Qiu et al., 2020). In order to further analyze the absorption mechanism of the CAA, we calculated the electromagnetic loss distribution of the designed optical structure at three specific wavelengths λ = 0.62 μm, λ = 1.11 μm and λ = 2.5 μm, and visualized in **Figure 2C**. It can be noted here that the overall loss of electromagnetic wave is distributed in the main absorption structure of C3/ZrC/C3, especially in the middle ZrC layer, and with the increase of incident wavelength, the electromagnetic wave would penetrate into the underlying layer resulting in the partial loss in the bottom ZrC layer.

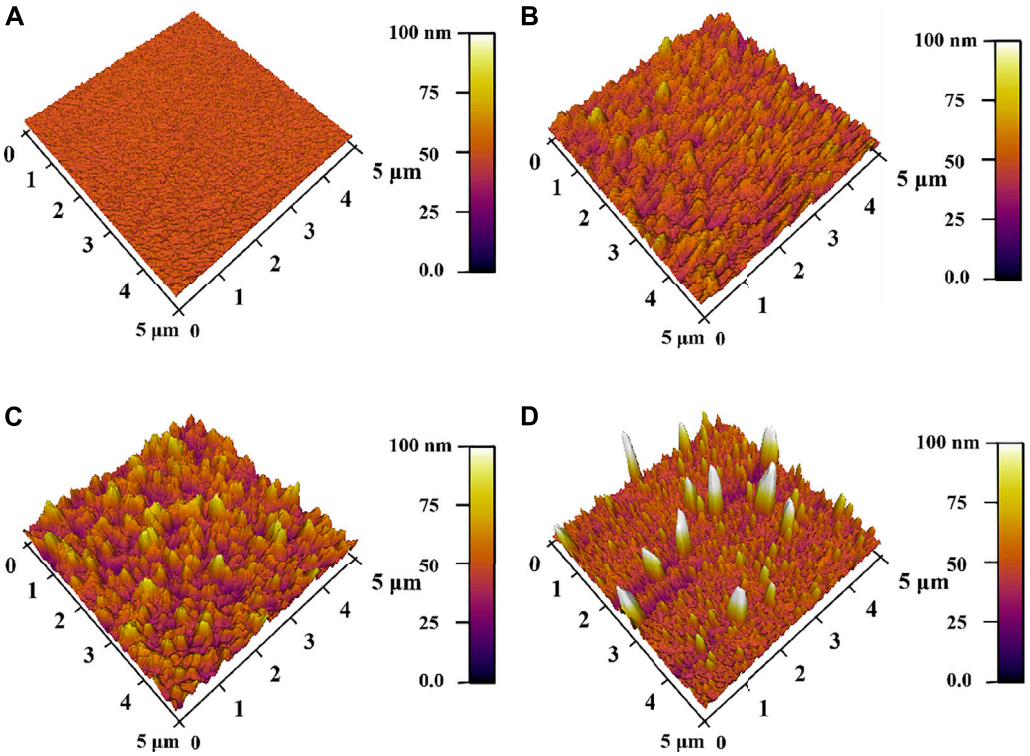

FIGURE 4 | Three-dimensional AFM images of the absorber CAA before annealing **(A)** and after annealing at 700°C **(B)**, 800°C **(C)**, and 900°C **(D)** in vacuum for 100 h.

TABLE 3 | Surface roughness of the absorber treated at different temperatures in vacuum.

Sample	SS	CAA	CAA-700	CAA-800	CAA-900
Temperature	_	_	700°C	800°C	900°C
Rq	0.2 nm	1.62 nm	6.2 nm	9.1 nm	11.3 nm

High-Temperature Properties of Selective Absorption Coatings

Enhancing the operating temperature of the spectrally selective absorber used in the CSP system would boost the conversion efficiency of solar energy to electricity. The as-deposited absorbers were treated in vacuum at different temperatures,

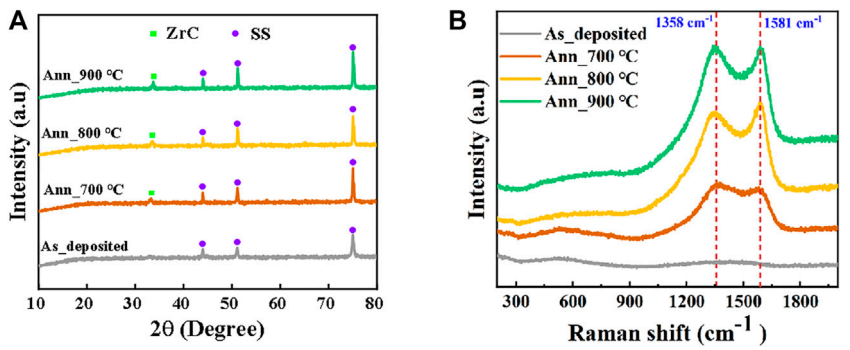

FIGURE 5 | XRD patterns **(A)** and Raman spectra **(B)** of CAA coatings deposited on stainless steel substrates before and after annealing at different temperatures in vacuum.

and the reflectance spectra of the coatings before and after annealing were shown in **Figure 3A**. Compared with the CAA before annealing, only negligible variations are observed in its reflectance spectra before the cutoff wavelength after annealing at 800°C and 900°C for 100 h, which testifies the superior thermal stability of the CAA even upon annealing in 900°C. Moreover, the calculated α and $\varepsilon_{82\ ^\circ C}$ of the CAA before and after annealing were summarized in **Figure 3B**. The CAA upon annealing still possesses a pretty high solar absorptance greater than 0.96. The improved reflectance of the CAA upon annealing in the thermal IR range is beneficial to the suppression of thermal emittance, which is due to the better crystallinity of the bottom infrared reflection layer ZrC after annealing. So, thermal emittance decreases from 0.160 to 0.143 with the increase of the annealed temperature. The photothermal conversion efficiency ($\eta_{thermal}$) of solar-to-heat and the total efficiency (η_{total}) of solar-to-electricity based on the CAA were calculated under different operating temperatures and optical concentrations using the following **Eqs 1–3**:

$$\eta_{Thermal} = \left[\alpha - \frac{\varepsilon\sigma\left(T_W^4 - T_{Amb}^4\right)}{C \cdot I_S}\right] \tag{1}$$

$$\eta_{Total} = \eta_{Thermal}\left(1 - \frac{T_{Amb}}{T_W}\right) = \left[\alpha - \frac{\varepsilon\sigma\left(T_W^4 - T_{Amb}^4\right)}{C \cdot I_S}\right]\left(1 - \frac{T_{Amb}}{T_W}\right) \tag{2}$$

$$\varepsilon = \frac{\int_{0.25um}^{20um}[1 - R(\lambda)] \cdot B(\lambda, T)d\lambda}{\int_{0.25um}^{20um} B(\lambda, T)d\lambda} \tag{3}$$

where T_W is the working temperature of the coating, T_{Amb} the ambient temperature, C the optical concentration factor, σ the Stefan-Boltzmann constant, and $B(\lambda,T)$ the black body emissive power at a certain temperature and wavelength. It should be noted here that the ε in **Eqs 1**, **2** is calculated by **Eq. 3** considering the temperature dependence of thermal emission. As shown in **Figure 3C**, the photothermal conversion coefficient increases with elevating the temperatures and can reach up to 91.4% under 1,000 suns and at 900°C, indicating the potential applications at high-temperature CSP system. **Figure 3D** depicts the total conversion efficiency including the photothermal conversion of the CAA and an ideal Carnot efficiency under different working temperatures and optical concentrations. There is an optimal total efficiency at the same optical concentration. A record-high total efficiency of 68% (1,000 suns) can be achieved at a reliable stable temperature (900°C) of the CAA.

Surface Morphology and Phase Analysis

In order to thoroughly comprehend the evolution behavior of the coating at high temperatures, the three-dimensional surface topography of the CAA before and after annealing at different temperatures was obtained and demonstrated in **Figure 4**. The grooves structure of the as-deposited CAA coating, shown in **Figure 1A** is attributed to the polished SS304 substrate and disappears after thermal treatment. Compared with the substrate, the roughness of the deposited coating increases but also remains at a low level of 1.62 nm, indicating excellent uniformity. As seen from **Figure 4B** to **Figure 4D**, when the coating CAA was respectively annealed at 700°C, 800°C, and 900°C for 100 h, the agglomeration phenomena appear and intensify with increasing the annealing temperature, together with the roughness increasing from 1.62 to 11.3 nm. More details on the coating roughness were summarized in **Table 3**. The change of the surface topography would affect the optical absorption of the absorber to a certain extent.

XRD was used to disclose the phase changes of the absorber CAA after long-term annealing at different temperatures. **Figure 5A** demonstrates XRD spectra of the CAA before and after heat treatment at 700°C, 800°C, and 900°C for 100 h. The pristine CAA (gray line) does not show any characteristic peaks of the coatings, except the peaks at 44°, 52°, and 77° connected with the traditional austenitic stainless steel substrate (Gualtieri and Bandyopadhyay 2017). In addition, a new peak was found at 33° on the annealed sample, which can be indexed to the ZrC (Schonfeld et al., 2017). The better crystallization of ZrC in the absorber upon annealing could be the reason for decreased thermal emittance in the annealed coatings compared with the pristine one. Similar to XRD patterns, the Raman spectra of the deposited coating do not show the sample signal peaks. However, after the heat treatment, the characteristic peaks of amorphous carbon (D and G peaks) appear at 1,358 cm^{-1} and 1,581 cm^{-1} (Gao et al., 2019a). The carbon aggregation from the substrate gradually strengthens with increasing the annealing temperatures. However, the aggregated carbons would not have a significant effect on the optical performances due to the introduction of the ultra-high temperature ceramics ZrC and the novel QOM structure. It can be predicted that choosing the stable dielectric substrate in the structure would further improve the thermal stability of the absorber at higher temperatures.

CONCLUSION

In summary, we designed and fabricated a heat-resisting and high-performance solar selective absorber CAA based on the ultra-high temperature ceramic ZrC on polished SS substrates. The as-deposited absorber exhibits outstanding spectral selectivity with a high absorptance of 96.4% and an IR emittance of 16%, which may be attributed to the sophisticated optical design coupled with multiple absorption mechanisms in the QOM structure and the introduction of ZrC. The absorbers can survive at 900°C for 100 h in vacuum, indicating superior thermal stability. The solar absorptance of the absorbers goes through a negligible change and remains at above 96% upon annealing, while thermal emittance decreases due to the better crystallization of ZrC beneficial for the suppression of heat loss. The photothermal efficiency of the absorber can reach 91.4% at the reliable operating temperature of 900°C and 1,000 suns. Eventually, a record-high total efficiency of 68% can be achieved when considering the ideal Carnot efficiency.

DATA AVAILABILITY STATEMENT

The original contributions presented in the study are included in the article/Supplementary Material, further inquiries can be directed to the corresponding authors.

AUTHOR CONTRIBUTIONS

JW: Investigation, Fabrication, Characterization, Formal Analysis, Writing Original Draft, and Reviewing. ZW: Methodology and Investigation. YL: Conceptualization and Investigation. SH: Reviewing. JM: Resources and Writing–Reviewing. XL: Writing–Reviewing. QZ: Resources and Writing–Reviewing. FC: Resources, Conceptualization, Editing, Reviewing, and Supervision. All authors approved the final version of the manuscript.

FUNDING

This work was funded by the National Natural Science Foundation of China (51871081 and 51971081), the Cheung Kong Scholar Reward Program Young Scholar Program of China (Q2018239), the Natural Science Foundation for Distinguished Young Scholars of Guangdong Province of China (2020B1515020023), Shenzhen Fundamental Research Program (GXWD20201230155427003-20200801190929005, and JCYJ20200109113418655), and Shenzhen Science and Technology Program (KQTD20200820113045081).

REFERENCES

Azad, A. K., Kort-Kamp, W. J. M., Sykora, M., Weisse-Bernstein, N. R., Luk, T. S., Taylor, A. J., et al. (2016). Metasurface Broadband Solar Absorber. *Sci. Rep.* 6, 6. doi:10.1038/srep20347

Cao, F., Kraemer, D., Sun, T., Lan, Y., Chen, G., and Ren, Z. (2015a). Enhanced Thermal Stability of W-Ni-Al2O3Cermet-Based Spectrally Selective Solar Absorbers with Tungsten Infrared Reflectors. *Adv. Energ. Mater.* 5 (2), 1401042. doi:10.1002/AENM.201401042

Cao, F., Kraemer, D., Tang, L., Li, Y., Litvinchuk, A. P., Bao, J., et al. (2015b). A High-Performance Spectrally-Selective Solar Absorber Based on a Yttria-Stabilized Zirconia Cermet with High-Temperature Stability. *Energy Environ. Sci.* 8 (10), 3040–3048. doi:10.1039/C5EE02066B

Cao, F., McEnaney, K., Chen, G., and Ren, Z. (2014). A Review of Cermet-Based Spectrally Selective Solar Absorbers. *Energ. Environ. Sci.* 7 (5), 1615–1627. doi:10.1039/C3EE43825B

Cao, F., Tang, L., Li, Y., Litvinchuk, A. P., Bao, J., and Ren, Z. (2017). A High-Temperature Stable Spectrally-Selective Solar Absorber Based on Cermet of Titanium Nitride in SiO2 Deposited on Lanthanum Aluminate. *Solar Energ. Mater. Solar Cell* 160, 12–17. doi:10.1016/j.solmat.2016.10.012

Chen, Y., Shen, C., Liu, Q., Hu, S., Zhou, X., and Xu, C. (2021). A Comparative Theoretical Study on the Structure Stability and Adhesion Properties of the Zr(0001)-ZrC(100) and Zr(0001)-ZrC(110) Interfaces. *Surf. Sci.* 713, 121895. doi:10.1016/j.susc.2021.121895

Chirumamilla, A., Yang, Y., Salazar, M. H., Ding, F., Wang, D., Kristensen, P. K., et al. (2021). Spectrally Selective Emitters Based on 3D Mo Nanopillars for Thermophotovoltaic Energy Harvesting. *Mater. Today Phys.* 21, 100503. doi:10.1016/j.mtphys.2021.100503

Fahrenholtz, W. G., and Hilmas, G. E. (2017). Ultra-high Temperature Ceramics: Materials for Extreme Environments. *Scripta Materialia* 129, 94–99. doi:10.1016/j.scriptamat.2016.10.018

Gao, X.-H., Qiu, X.-L., Li, X.-T., Theiss, W., Chen, B.-H., Guo, H.-X., et al. (2019b). Structure, thermal Stability and Optical Simulation of ZrB2 Based Spectrally Selective Solar Absorber Coatings. *Solar Energ. Mater. Solar Cell* 193, 178–183. doi:10.1016/j.solmat.2018.12.040

Gao, X.-H., Qiu, X.-L., Shen, Y.-Q., He, C.-Y., and Liu, G. (2019a). A Novel TiC-ZrB_2/ZrB_2/Al_2O_3 Multilayer High Temperature Solar Selective Absorbing Coating: Microstructure, Optical Properties and Failure Mechanism. *Solar Energ. Mater. Solar Cell* 203, 110187. doi:10.1016/J.SOLMAT.2019.110187

Gualtieri, T., and Bandyopadhyay, A. (2017). Niobium Carbide Compostie Coatings on SS304 Using Laser Engineered Net Shaping (LENS™). *Mater. Lett.* 189, 89–92. doi:10.1016/j.matlet.2016.11.071

He, C.-Y., Gao, X.-H., Qiu, X.-L., Yu, D.-M., Guo, H.-X., and Liu, G. (2021a). Scalable and Ultrathin High-Temperature Solar Selective Absorbing Coatings Based on the High-Entropy Nanoceramic AlCrWTaNbTiN with High Photothermal Conversion Efficiency. *Sol. RRL* 5 (4), 2000790. doi:10.1002/solr.202000790

He, C.-Y., Gao, X.-H., Yu, D.-M., Qiu, X.-L., Guo, H.-X., and Liu, G. (2021b). Scalable and Highly Efficient High Temperature Solar Absorber Coatings Based on High Entropy alloy Nitride AlCrTaTiZrN with Different Antireflection Layers. *J. Mater. Chem. A.* 9 (10), 6413–6422. doi:10.1039/d0ta09988k

Hoch, L. B., O'Brien, P. G., Jelle, A., Sandhel, A., Perovic, D. D., Mims, C. A., et al. (2016). Nanostructured Indium Oxide Coated Silicon Nanowire Arrays: A Hybrid Photothermal/Photochemical Approach to Solar Fuels. *ACS Nano* 10 (9), 9017–9025. doi:10.1021/acsnano.6b05416

Jiasheng, R. (1996). The Use and Development of Solar Energy. *J. Electron. Devices (China)* 19 (4), 292–297.

Kan, A., Zeng, Y., Meng, X., Wang, D., Xina, J., Yang, X., et al. (2021). The Linkage between Renewable Energy Potential and Sustainable Development: Understanding Solar Energy Variability and Photovoltaic Power Potential in Tibet, China. *Sustainable Energ. Tech. Assessments* 48, 101551. doi:10.1016/j.seta.2021.101551

Li, Y., Lin, C., Wu, Z., Chen, Z., Chi, C., Cao, F., et al. (2021). Solution-Processed All-Ceramic Plasmonic Metamaterials for Efficient Solar-Thermal Conversion over 100-727 °C. *Adv. Mater.* 33 (1), 2005074. doi:10.1002/adma.202005074

Liang, Q., Fu, Y., Xia, X., Wang, L., and Gao, R. (2018). Titanium Nitride Nano-Disk Arrays-Based Metasurface as a Perfect Absorber in the Visible Range. *Mod. Phys. Lett. B* 32 (1), 1750365. doi:10.1142/s0217984917503651

Liu, Y., Wu, Z., Yin, L., Zhang, Z., Wu, X., Wei, D., et al. (2019). High-temperature Air-Stable Solar Absorbing Coatings Based on the Cermet of $MoSi_2$ Embedded in SiO_2. *Solar Energ. Mater. Solar Cell* 200, 109946. doi:10.1016/J.SOLMAT.2019.109946

Meng, J.-p., Liu, X.-p., Fu, Z.-q., and Zhang, K. (2017). Optical Design of Cu/$Zr_{0.2}AlN_{0.8}$/ZrN/AlN/ZrN/AlN/$Al_{34}O_{62}N_4$ Solar Selective Absorbing Coatings. *Solar Energy* 146, 430–435. doi:10.1016/j.solener.2017.03.012

Meng, J.-P., and Zhou Li, L. (2019). Enhanced thermal Stability of ZrAlSiN Cermet-Based Solar Selective Absorbing Coatings *via* Adding Silicon Element. *Mater. Today Phys.* 9, 100131. doi:10.1016/j.mtphys.2019.100131

Ning, Y., Wang, W., Sun, Y., Wu, Y., Liu, Y., Man, H., et al. (2016). Effects of Substrates, Film Thickness and Temperature on thermal Emittance of Mo/substrate Deposited by Magnetron Sputtering. *Vacuum* 128, 73–79. doi:10.1016/j.vacuum.2016.03.008

Okuhara, Y., Kuroyama, T., Yokoe, D., Kato, T., Takata, M., Tsutsui, T., et al. (2018). High-temperature Solar-thermal Conversion by Semiconducting β-$FeSi_2$ Absorbers with Thermally Stabilized Silver Layers. *Solar Energ. Mater. Solar Cell* 174, 351–358. doi:10.1016/j.solmat.2017.09.023

Qiu, X.-L., Gao, X.-H., He, C.-Y., and Liu, G. (2020). Optical Design, thermal Shock Resistance and Failure Mechanism of a Novel Multilayer Spectrally Selective Absorber Coating Based on HfB_2 and ZrB_2. *Solar Energ. Mater. Solar Cell* 211, 110533. doi:10.1016/J.SOLMAT.2020.110533

Rosenbaum, M., Schröder, U., and Scholz, F. (2005). *In Situ* electrooxidation of Photobiological Hydrogen in a Photobioelectrochemical Fuel Cell Based on Rhodobacter Sphaeroides. *Environ. Sci. Technol.* 39 (16), 6328–6333. doi:10.1021/es0505447

Schönfeld, K., Martin, H.-P., and Michaelis, A. (2017). Pressureless Sintering of ZrC with Variable Stoichiometry. *J. Adv. Ceram.* 6 (2), 165–175. doi:10.1007/s40145-017-0229-1

Tang, S., and Hu, C. (2017). Design, Preparation and Properties of Carbon Fiber Reinforced Ultra-high Temperature Ceramic Composites for Aerospace Applications: A Review. *J. Mater. Sci. Tech.* 33 (2), 117–130. doi:10.1016/j.jmst.2016.08.004

Turon, V., Ollivier, S., Cwicklinski, G., Willison, J. C., and Anxionnaz-Minvielle, Z. (2021). H-2 Production by Photofermentation in an Innovative Plate-type Photobioreactor with Meandering Channels. *Biotechnol. Bioeng.* 118 (3), 1342–1354. doi:10.1002/bit.27656

Vidal, J. C., and Klammer, N. (2019). "Molten Chloride Technology Pathway to Meet the US DOE SunShot Initiative with Gen3 CSP," in *Solarpaces 2018: International Conference on Concentrating Solar Power and Chemical Energy Systems*. Editor C. Richter (Melville: Amer Inst Physics). doi:10.1063/1.5117601

Wang, J., Ren, Z., Luo, Y., Wu, Z., Liu, Y., Hou, S., et al. (2021a). High-Performance Spectrally Selective Absorber Using the ZrB_2-Based All-Ceramic Coatings. *ACS Appl. Mater. Inter.* 13 (34), 40522–40530. doi:10.1021/acsami.1c08947

Wang, S., Cao, F., Wu, Y., Zhang, X., Zou, J., Lan, Z., et al. (2021). Multifunctional 2D Perovskite Capping Layer Using Cyclohexylmethylammonium Bromide for Highly Efficient and Stable Perovskite Solar Cells. *Mater. Today Phys.* 21, 100543. doi:10.1016/j.mtphys.2021.100543

Wang, X., Gao, J., Hu, H., Zhang, H., Liang, L., Javaid, K., et al. (2017). High-temperature Tolerance in WTi-Al_2O_3 Cermet-Based Solar Selective Absorbing Coatings with Low thermal Emissivity. *Nano Energy* 37, 232–241. doi:10.1016/j.nanoen.2017.05.036

Wang, X., Lee, E., Xu, C., and Liu, J. (2021). High-efficiency, Air-Stable Manganese-Iron Oxide Nanoparticle-Pigmented Solar Selective Absorber Coatings toward Concentrating Solar Power Systems Operating at 750 °C. *Mater. Today Energ.* 19, 100609. doi:10.1016/j.mtener.2020.100609

Wei, D., Cao, F., Wu, Z., Liu, Y., Wang, J., Wang, Q., et al. (2021). Enhanced Spectral Splitting in a Novel Solar Spectrum Optical Splitter Based on One Dimensional Photonic crystal Heterostructure. *J. Materiomics* 7, 648–655. doi:10.1016/J.JMAT.2020.10.014

Weinstein, L. A., Loomis, J., Bhatia, B., Bierman, D. M., Wang, E. N., and Chen, G. (2015). Concentrating Solar Power. *Chem. Rev.* 115, 12797–12838. doi:10.1021/ACS.CHEMREV.5B00397

Wu, Z., Liu, Y., Wei, D., Yin, L., Bai, F., Liu, X., et al. (2019). Enhanced Spectral Selectivity through the Quasi-Optical Microcavity Based on W-SiO2 Cermet. *Mater. Today Phys.* 9, 100089. doi:10.1016/j.mtphys.2019.03.003

Wu, Z., Wang, J., Liu, Y., Hou, S., Liu, X., Zhang, Q., et al. (2021). A Review of Spectral Controlling for Renewable Energy Harvesting and Conserving. *Mater. Today Phys.* 18, 100388. doi:10.1016/j.mtphys.2021.100388

Wu, Z., Xue, W., Liu, Y., Wei, D., Wang, J., Yin, L., et al. (2020). Toward Versatile Applications *via* Tuning Transition Wavelength of the WTa-SiO_2 Based Spectrally Selective Absorber. *Solar Energy* 202, 115–122. doi:10.1016/J.SOLENER.2020.03.051

Yang, D., Zhao, X., Liu, Y., Li, J., Liu, H., Hu, X., et al. (2020). Enhanced thermal Stability of Solar Selective Absorber Based on Nano-Multilayered AlCrSiO Films. *Solar Energ. Mater. Solar Cell* 207, 110331. doi:10.1016/j.solmat.2019.110331

Yang, J., Shen, H., Yang, Z., and Gao, K. (2021). Air-Stability Improvement of Solar Selective Absorbers Based on TiW-SiO_2 Cermet up to 800 °C. *ACS Appl. Mater. Inter.* 13 (12), 14587–14598. doi:10.1021/acsami.1c00594

Yushchenko, A., de Bono, A., Chatenoux, B., Kumar Patel, M., and Ray, N. (2018). GIS-based Assessment of Photovoltaic (PV) and Concentrated Solar Power (CSP) Generation Potential in West Africa. *Renew. Sust. Energ. Rev.* 81, 2088–2103. doi:10.1016/j.rser.2017.06.021

Zhang, K., Du, M., Hao, L., Meng, J., Wang, J., Mi, J., et al. (2016). Highly Corrosion Resistant and Sandwich-like Si_3N_4/Cr-CrNx/Si_3N_4 Coatings Used for Solar Selective Absorbing Applications. *ACS Appl. Mater. Inter.* 8 (49), 34008–34018. doi:10.1021/acsami.6b11607

Conflict of Interest: The authors declare that the research was conducted in the absence of any commercial or financial relationships that could be construed as a potential conflict of interest.

Publisher's Note: All claims expressed in this article are solely those of the authors and do not necessarily represent those of their affiliated organizations, or those of the publisher, the editors and the reviewers. Any product that may be evaluated in this article, or claim that may be made by its manufacturer, is not guaranteed or endorsed by the publisher.